



HHS Public Access

Author manuscript

Bioconjug Chem. Author manuscript; available in PMC 2018 June 07.

Published in final edited form as:

Bioconjug Chem. 2017 May 17; 28(5): 1560–1565. doi:10.1021/acs.bioconjchem.7b00201.

IFacile quenching and spatial patterning of cyclooctynes via strain-promoted alkyne–azide cycloaddition of inorganic azides

Matthew Bjerknes^{†,*}, Hazel Cheng[†], Christopher D. McNitt[‡], and Vladimir V. Popik^{‡,*}

[†]Departments of Medicine and Medical Biophysics, University of Toronto, Toronto, Ontario M5S 1A8, Canada

[‡]Department of Chemistry, University of Georgia, Athens, Georgia 30602, United States

Abstract

Little is known about the reactivity of strain-promoted alkyne–azide cycloaddition (SPAAC) reagents with inorganic azides. We explore the reactions of a variety of popular SPAAC reagents with sodium azide and hydrozoic acid. We find that the reactions proceed in water at rates comparable to those with organic azides, yielding in all cases a triazole adduct. The azide ion's utility as a cyclooctyne quenching reagent is demonstrated by using it to spatially pattern uniformly-doped hydrogels. The facile quenching of cyclooctynes demonstrated here should be useful in other bioorthogonal ligation techniques in which cyclooctynes are employed, including SPANC, Diels-Alder, and thiol-yne.

INTRODUCTION

Inorganic azides have long been known to react with alkynes, but the reaction is generally inefficient, requiring heat or catalysts. An early example is the cycloaddition of hydrazoic acid to acetylene, which upon heating yields un-substituted NH-1,2,3-triazole.¹ The reluctant reactivity of sodium azide with alkynes, due to a large activation enthalpy², is the basis of the success of the one-pot, two-step synthesis scheme^{3,4} in which sodium azide first reacts with an organic halide, yielding an organic azide that in a second step reacts with an alkyne via a Cu(I)-Catalyzed Azide–Alkyne Cycloaddition (CuAAC) reaction to generate the desired triazole, often in high yield. However, it was also noted that if the nucleophilic substitution of the halide is inefficient, then formation of an NH-triazole can occur as an undesired side reaction.⁴

More recently, Wang et al.^{5,6} described two novel cyclooctyne strain-promoted alkyne–azide cycloaddition (SPAAC) reagents useful as probes for detecting inorganic azide contaminants in solutions. Their results demonstrated that some SPAAC reagents can undergo a slow

*Corresponding Author: matthew.bjerknes@utoronto.ca, vpopik@uga.edu.

Author Contributions

The manuscript was written through contributions of all authors. All authors have given approval to the final version of the manuscript.

Supporting Information. The Supporting Information is available free of charge on the ACS Publications website at DOI: to be determined. Experimental procedures, including synthesis, reaction conditions and kinetics, hydrogel preparation, and spectral measurement procedures; derivation of the competitive kinetics calculation for BCN reaction kinetics; additional figures demonstrating photo-ODIBO and ODIBO triazole stability (PDF).

reaction with sodium azide, but it remains unclear whether this is a distinctive feature of their specialized SPAAC reagents or whether SPAAC reactivity with inorganic azides is a general and potentially useful class of reactions.

In the years since Agard et al.⁷ introduced SPAAC as a copper-free 'click reaction' for protein labeling, many novel reagents have been developed, often in an attempt to enhance the azide reactivity and stability of cyclooctynes.⁸ The specificity and convenience of the cycloaddition reaction with an essentially limitless variety of organic azides has led to a steadily growing range of applications of SPAAC reagents in chemical synthesis and biology, usually as a selective conjugation tool. The popular SPAAC reagents ODIBO⁹, ADIBO^{10,11} (a.k.a DIBAC¹² or DBCO), DIBO¹³, and BCN¹⁴ are known to differ dramatically in their respective reaction rates with organic azides^{9,10,13,15}, but little is known about their reactivity with inorganic azides. Our interest in SPAAC reactivity with inorganic azides was provoked by the intermittent failure of a cyclooctyne labeling experiment. The culprit was identified as sodium azide, often used as a preservative in commercial antibodies, and the failure was found to be due to an efficient SPAAC reaction with the azide ion, effectively quenching the cyclooctyne by generating the triazole.

Scheme 1 provides a conceptual overview of the paper. We first characterize in detail the reaction of a variety of cyclooctynes with azide ion (Schemes 2–4), including measurements of the reaction kinetics and the chemical identification of the resulting products. Then we demonstrate that cyclopropanones and triazoles do not react with azide ions, allowing its use in quenching undesired background cyclooctynes without negatively impacting subsequent photopatterning applications. Then we illustrate the utility of the reaction with azide ions in patterning the conjugation of azide-coupled molecules to a hydrogel substrate.

The characterization of the general SPAAC reactivity with inorganic azides reported here adds an inexpensive, flexible, and effective quenching alternative to the use of low molecular weight organic azides (requiring organic solvents) or large expensive water soluble azides such as the PEG-azides.

RESULTS AND DISCUSSION

We found that each of the cyclooctynes of Scheme 2 readily reacts with sodium azide in PBS (containing 5% MeOH for cyclooctyne solubility) at pH = 7.4. HPLC analysis of the reaction mixtures starting with **2** or **4** showed complete consumption of the cyclooctyne and the formation of a single product in the reactions¹⁵. HRMS analysis¹⁵ confirmed that a single triazole product was formed in each of these two reactions (**5** and **6** of Scheme 3, respectively). However, two products were observed chromatographically when a p-iodobenzoate derivative of DIBO (DIBO-IBA, **3a**) was reacted with sodium azide. Triazoles **7a** and **7b** were isolated in 79% and 19% yields, respectively, from a subsequent preparative reaction of **3a** with equimolar sodium azide (Scheme 3). In the absence of azide ion, **3a** and **7a** were stable under ambient conditions in either PBS (containing 5% methanol) or in pure methanol. Therefore, since triazole **7b** is the apparent product of phenyl ester hydrolysis, this indicates that the azide ion can act as a nucleophilic catalyst of cleavage of the otherwise stable ester. The 98% preparative yield of triazoles **7a,b** indicates that 1,3-dipolar

cycloaddition of the azide ion across the triple bond of dibenzocyclooctynes **2–4** proceeds quantitatively.

A single triazole product (**8**) resulted from the reaction of sodium azide with ODIBO (**1**) at azide concentrations below 50 mM. However, at higher azide concentrations two minor by-products were observed by HPLC in addition to the major adduct **8**. In a scaled-up reaction, we managed to isolate 53% of the triazole **8** and 20% of the methyl vinyl ether **9**, the latter the apparent product of methanol addition across the triple bond (Scheme 4).¹⁵ The second byproduct decomposes on the silica gel column during separation, but by analogy with the formation of **9**, we suggest that it is produced by the hydration of **1** in the course of the reaction.

It is interesting to note, that triazole **8** and cyclooctyne **1** are stable in PBS with 5% methanol, their UV spectra¹⁵ showing no signs of decomposition after overnight incubation and no detectable amounts of **9** were seen by HPLC. This observation suggests that azide ion somehow catalyzes the methanol addition across the triple bond

The NMR spectral features¹⁵ of triazoles **7** and **8** are insufficient to assign a *1H*- versus *2H*-triazole structure.¹⁶ Nonetheless, we have assigned the *2H*-triazole structure because we found that the addition of butyl azide to ODIBO **1** results in the formation of two regioisomeric 1-butyl-*1H*-triazoles (head-to-head and head-to-tail adduct).¹⁵ The isomers are readily resolved by HPLC and produce different NMR spectra. We reasoned that two isomers would have similarly resulted if the addition of the azide ion or hydrazoic acid to ODIBO also yielded a *1H*-triazole; however HPLC reveals only a single triazole product from this reaction, as well as from the DIBO-IBA (**3a**) reaction. In addition, NMR spectra of **7a,b** and **8** show no doubling of any signals. Therefore, it is reasonable to assign a *2H*-structure to both triazoles **7** and **8**.

Kinetics of cycloaddition reactions with azide ion and hydrazoic acid

The progress of the reaction was followed by the disappearance of the characteristic UV absorbance of dibenzocyclooctynes **1–3**, as illustrated for ODIBO (**1**) in Figure 1. The consumption of ODIBO (**1**) was followed by measuring the decay of its characteristic band at 321 nm, while the band at 309 nm was measured for ADIBO (**2**) and DIBO (**3**). Similar spectral changes were observed in reactions of cyclooctynes **1–3** with hydrazoic acid at pH=1.¹⁵ The reactions were performed at 25.0±0.1 °C, using a 10 fold or higher excess of sodium azide to ensure pseudo-first order conditions, and hence improved accuracy of the resulting rate estimates. A single product was seen by HPLC in each case, under the conditions used for the kinetics reactions.

The experimental data were well-fit by a single exponential decay model, providing estimates of the pseudo-first order rate constants at each sodium azide concentration (Figure 2). The observed rates, k_{obs} , showed a linear dependence on the azide concentration (Figures 3 and 4). The bimolecular rate constants presented in Table 1 are the slopes estimated from the data by linear regression.

A different strategy was necessary to estimate the reaction rate for BCN (**4**) since it has no significant absorbance above 250 nm. Instead, BCN reaction rates with azide ion and hydrazoic acid were estimated using pseudo-first order competition experiments with DIBO as described in the supplement (**3b**, Table 1).

The reactivity of cyclooctynes **1–4** towards the azide ion and hydrazoic acid is correlated with their respective reactivity in the cycloaddition of organic azides (Table 1; Scheme 2)^{9,10,13,15}. It is also interesting to note that the polarity of the alkyne seems to impact its reactivity with hydrazoic acid in comparison to azide ion. Thus hydrazoic acid is about five fold less reactive than azide ion in 1,3-dipolar cycloaddition to cyclooctynes whose triple bond is polarized (**1** and **2**), but more reactive than azide ion in reactions with cyclooctynes whose triple bond is non-polarized (**3** and **4**).

Stability of cyclopropanones and triazoles

No decomposition was detected following incubation of photo-ODIBO-TEG (**S2**) in the presence of 25 mM sodium azide at 25°C in PBS containing 5% of methanol for 24 h (Figure S1).¹⁵ Triazole **8** was also found to be stable under neutral conditions and in 0.1 M perchloric acid (Figure S2). It also does not react with sodium azide under these conditions.

Quenching and patterning

Our results show that azide ions are potent general purpose cyclooctyne quenching reagents, resulting in the formation of stable triazole. The stability of the resulting triazoles prompted us to explore the utility of azide ions in patterning model biomaterials. We tested using azide ion quenching to generate a pattern of molecules attached to a hydrogel scaffold. We used 6-carboxyfluorescein-TEG-azide as a reporter, but any azide coupled molecule of interest could be similarly patterned into a hydrogel, including growth factors, adhesion factors, or drugs.

We first made a polyacrylamide hydrogel doped with allylamine as a source of primary amine to which we coupled photo-ODIBO-TEG-NHS (**10**)¹⁵, resulting in a uniform field of photo-ODIBO, the light-activated precursor of ODIBO (Scheme 5, Figure 5). This was converted to a uniform field of ODIBO by exposure to 350 nm light (Scheme 5). We then applied a solution of 20 mM NaN₃ to one end of the hydrogel, and allowed it to migrate into the gel overnight, quenching ODIBO as it migrated along the gel. The formation of a spatial gradient of ODIBO along the gel was confirmed by direct spot measurements of the absorbance spectrum of the gel (Figure 5). The gel was then reacted with 6-carboxyfluorescein-TEG azide, which yielded a fluorescein gradient across the gel that was seen by absorbance spectroscopy and fluorescence imaging (Figure 5).

Quenching and negative photopatterning

Negative photopatterning provides a second example of the utility of azide ion quenching. We prepared a hydrogel doped with a uniform field of photo-ODIBO as above (Figure 6A). We then projected the image of an iris diaphragm onto the hydrogel with 350 nm light. The resulting decarbonylation reaction within the illuminated disk generated a spot of ODIBO in the previously uniform field of photo-ODIBO. The ODIBO in the imaged disk was then

quenched by washing the whole hydrogel sample with sodium azide. The background photo-ODIBO in the remainder of the hydrogel was unaffected, as expected from our observation that photo-ODIBO is stable in azide ions (Figure S1). A second image of the diaphragm was then projected onto an adjacent region of the hydrogel. This time, the gel was washed with Rhodamine B-azide, which reacted with the ODIBO in the second image of the diaphragm. Any residual ODIBO was then quenched by a second azide ion wash. Finally, the entire gel was uniformly irradiated with 350 nm light to generate a field of ODIBO in the surrounding unexposed areas of the hydrogel. The resulting global background of ODIBO was then labeled by washing the hydrogel with 6-carboxyfluorescein-TEG-azide. The final product is a hydrogel with a green fluorescent background surrounding the red fluorescent (Rhodamine B) and dark (azide ion-quenched) images of the projected diaphragm (Figure 6B). The black spot indicates the successful quenching of ODIBO by NaN_3 , and confirms that the products of the quenching reaction are relatively non-reactive with subsequently applied organic azides (in this case, 6-carboxyfluorescein-TEG-azide and Rhodamine B-azide).

CONCLUSIONS

Each of the SPAAC reagents tested reacted readily with inorganic azide ions, yielding the respective triazole. In addition, at higher concentrations, the dibenzocyclooctynes also yielded various side reactions likely catalyzed by the azide ion. Importantly, both the primary triazoles and the side products were unreactive with organic azides ensuring complete quenching of reactivity in downstream applications. This may be useful when there is a need to quench excess or contaminating cyclooctyne in preparation for downstream reactions, for example, in sequential click ligation of azide-tagged substrates,^{17–22} surface patterning,²³ or layer-by-layer derivatization²⁴. For example, SPAAC reagents are known to react slowly with thiol groups, resulting in non-specific labelling in many applications²⁵. Sodium azide quenching provides a potentially useful means of alleviating this common problem. By such facile quenching of the residual cyclooctyne before initiating a second SPAAC or CuAAC reaction, unwanted homo-coupled byproducts can be avoided. Cyclooctynes are also employed in other bioorthogonal ligation reactions – including SPAAC, SPANC, Diels-Alder, and thiol-yne – and hence the facile cyclooctyne quenching reaction described here has utility beyond SPAAC-based techniques.

It is important to emphasize that we have shown that cyclooctynes react with azide ion, but that cyclopropenone-caged light-activated precursors do not. This discrimination is very useful in quenching the former without affecting the latter. Thus, for example, undesired background cyclooctynes can be easily and specifically quenched.

The relative reactivity of each SPAAC reagent with inorganic azide correlates with its reactivity with organic azide. Thus quenching of slow-reacting SPAAC reagents is comparatively slow; however, quenching reactions can be accelerated to some extent by simply increasing the azide ion concentration.

SPAAC chemistry has proven to be a powerful approach to the derivatization of hydrogels, which are used for studying cell-substrate interaction^{26–29}. The facile quenching with azide ions demonstrated here should ease many applications of the method. The coupling of a

light-activated SPAAC reagent to an amine-doped hydrogel as demonstrated here provides a model of negative spatial patterning using azide ions, either alone or in concert with patterned photoactivation. The resulting negative patterning may frequently be helpful in generating complex patterns, adding a complementary tool to the powerful photo-patterning toolkit^{31–33}. Potential applications include the patterning of hydrogels using SPAAC reagents with azide-conjugated bioactive reagents such as growth or cell adhesion factors, for use in cell cultures^{28–30}.

Supplementary Material

Refer to Web version on PubMed Central for supplementary material.

Acknowledgments

We are grateful for funding provided by Ontario Genomics under the SPARK program (M.B. and H.C.), and the National Science Foundation (CHE-1565646, V.P.).

References

1. Dimroth O, Fester G. Triazole and tetrazole from hydrazoic acid (Engl. Transl.). *Berichte der Deutschen Chemischen Gesellschaft*. 1910; 43:2219–2223.
2. Jones GO, Ess DH, Houk KN. Activation energies and reaction energetics for 1,3-dipolar cycloadditions of hydrazoic acid with C—C and C—N multiple bonds from high-accuracy and density functional quantum mechanical calculations. *Helv Chim Acta*. 2005; 88:1702–1710.
3. Maksikova AV, Serebryakova ES, Tikhonova LG, Vereshagin LI. Synthesis of 1-alkyl-4 (5)-hydroxymethyl-1,2,3-triazoles. *Chem Heterocycl Comp (Engl Transl)*. 1980:1284–1285. *Khimiya Geterotsiklicheskikh Soedinenii*. 12:1688–1689.
4. Feldman AK, Colasson B, Fokin VV. One-pot synthesis of 1,4-disubstituted 1,2,3-triazoles from in situ generated azides. *Org Lett*. 2004; 6:3897–3899. [PubMed: 15496058]
5. Wang L, Dai C, Chen W, Wang SL, Wang B. Facile derivatization of azide ions using click chemistry for their sensitive detection with LC-MS. *Chem Commun*. 2011; 47:10377–10379.
6. Wang K, Friscourt F, Dai C, Wang L, Zheng Y, Boons GJ, Wang S, Wang BA. A metal-free turn-on fluorescent probe for the fast and sensitive detection of inorganic azides. *Bioorg Med Chem Lett*. 2016; 26:1651–1654. [PubMed: 26944613]
7. Agard NJ, Prescher JA, Bertozzi CR. A strain-promoted [3 + 2] azide alkyne cycloaddition for covalent modification of biomolecules in living systems. *J Am Chem Soc*. 2004; 126:15046–15047. [PubMed: 15547999]
8. Dommerholt J, Rutjes FPJT, van Delft FL. Strain-promoted 1, 3-dipolar cycloaddition of cycloalkynes and organic azides. *Top Curr Chem (Z)*. 2016; 374:16.
9. McNitt CD, Popik VV. Photochemical generation of oxa-dibenzocyclooctyne (ODIBO) for metal-free click ligations. *Org Biomol Chem*. 2012; 10:8200–8202. [PubMed: 22987146]
10. Kuzmin A, Poloukhine A, Wolfert MA, Popik VV. Surface functionalization using catalyst-free azide alkyne cycloaddition. *Bioconjugate Chem*. 2010; 21:2076–2085.
11. Orski S, Sheppard GR, Arumugam S, Popik VV, Locklin J. Rate determination of azide click reactions onto alkyne polymer brush scaffolds: a comparison of conventional and catalyst-free cycloadditions for tunable surface modification. *Langmuir*. 2012; 28:14693–14702. [PubMed: 23009188]
11. Debets MF, van Berkel SS, Schoffelen S, Rutjes FPJT, van Hest MJC, van Delft FL. Aza-dibenzocyclooctynes for fast and efficient enzyme PEGylation via copper-free (3+2) cycloaddition. *Chem Commun*. 2010; 46:97–99.
12. Poloukhine AA, Mbua NE, Wolfert MA, Boons GJ, Popik VV. Selective labeling of living cells by a photo-triggered click reaction. *J Am Chem Soc*. 2009; 131:15769–15776. [PubMed: 19860481]

13. Dommerholt J, Schmidt S, Temming R, Hendriks LJA, Rutjes FPJT, van Hest JCM, Lefebber DJ, Friedl P, van Delft FL. Readily accessible bicyclononynes for bioorthogonal labeling and three-dimensional imaging of living cells. *Angew Chem Int Ed.* 2010; 49:9422–9425.
14. Supporting information.
15. Belskaya N, Subbotina J, Lesogorova S. Synthesis of 2H-1,2,3-triazoles. *Top Heterocycl Chem.* 2014; 40:51–116.
16. Chan DPY, Owen SC, Shoichet MS. Double click: dual functionalized polymeric micelles with antibodies and peptides. *Bioconjugate Chem.* 2013; 24:105–113.
17. Beal DM, Albrow VE, Burslem G, Hitchen L, Fernandes C, Laphorn C, Roberts LR, Selby MD, Jones LH. Click-enabled heterotrifunctional template for sequential bioconjugations. *Org Biomol Chem.* 2012; 10:548–554. [PubMed: 22101938]
18. Sutton AD, Popik VV. Sequential photochemistry of dibenzo[a,e]dicyclopropa[c,g][8]annulene-1,6-dione: selective formation of didehydridibenzo[a,e][8]annulenes with ultrafast SPAAC reactivity. *J Org Chem.* 2016; 81:8850–8857. [PubMed: 27635662]
19. Arumugam S, Popik VV. Sequential “click” – “photo-click” cross-linker for catalyst-free ligation of azide-tagged substrates. *J Org Chem.* 2014; 79:2702–2708. [PubMed: 24548078]
20. Zong H, Goonewardena SN, Chang HN, Otis JB, Baker JRJ. Sequential and parallel dual labeling of nanoparticles using click chemistry. *Bioorg Med Chem.* 2014; 22:6288–6296. [PubMed: 25257910]
21. Lai CH, Chang TC, Chuang YJ, Tzou DL, Lin CC. Stepwise orthogonal click chemistry toward fabrication of paclitaxel/galactose functionalized fluorescent nanoparticles for HepG2 cell targeting and delivery. *Bioconjugate Chem.* 2013; 24:1698–1709.
22. Orski SV, Poloukhine AA, Arumugam S, Mao L, Popik VV, Locklin J. High density orthogonal surface immobilization via photoactivated copper-free click chemistry. *J Am Chem Soc.* 2010; 132:11024–6. [PubMed: 20698664]
23. Münster N, Nikodemiak P, Koert U. Chemoselective layer-by-layer approach utilizing click reactions with ethynylcyclooctynes and diazides. *Org Lett.* 2016; 18:4296–4299. [PubMed: 27537081]
24. van Geel R, Pruijn GJM, van Delft FL, Boelens WC. Preventing thiol-yne addition improves the specificity of strain-promoted azide–alkyne cycloaddition. *Bioconjugate Chem.* 2012; 23:392–398.
25. DeForest CA, Sims EA, Anseth KS. Peptide-functionalized click hydrogels with independently tunable mechanics and chemical functionality for 3D cell culture. *Chem Mater.* 2010; 22:4783–4790. [PubMed: 20842213]
26. Okano K, Hsu HY, Li YK, Masuhara H. *In situ* patterning and controlling living cells by utilizing femtosecond laser. *J Photochem Photobiol C.* 2016; 28:1–28.
27. Zheng J, Smith Callahan LA, Hao J, Guo K, Wesdemiotis C, Weiss RA, Becker ML. Strain-promoted cross-linking of peg-based hydrogels via copper-free cycloaddition. *ACS Macro Lett.* 2012; 1:1071–1073. [PubMed: 23205321]
28. Ham, TR., Farrag, M., Leipzig, ND. Covalent growth factor tethering to direct neural stem cell differentiation and self-organization. *Acta Biomater.* 2017. <http://dx.doi.org/10.1016/j.actbio.2017.01.068>
29. Jiang Y, Chen J, Deng C, Suuronen EJ, Zhong Z. Click hydrogels, microgels and nanogels: Emerging platforms for drug delivery and tissue engineering. *Biomater.* 2014; 35:4969–4985.
30. Wang X, Li Z, Shi T, Zhao P, An K, Lin C, Liu H. Injectable dextran hydrogels fabricated by metal-free click chemistry for cartilage tissue engineering. *Mat Sci Eng C* 2017. 2017; 73:21–30.
31. Tang W, Becker ML. “Click” reactions: a versatile toolbox for the synthesis of peptide-conjugates. *Chem Soc Rev.* 2014; 43:7013–7039. [PubMed: 24993161]
32. Peppas NA, Khademhosseini A. Make better, safer biomaterials. *Nature.* 2016; 540:335–337. [PubMed: 27974790]
33. Delaittre G, Goldmann AS, Mueller JO, Barner-Kowollik C. Efficient photochemical approaches for spatially resolved surface functionalization. *Angew Chem Int Ed.* 2015; 54:11388–11403.

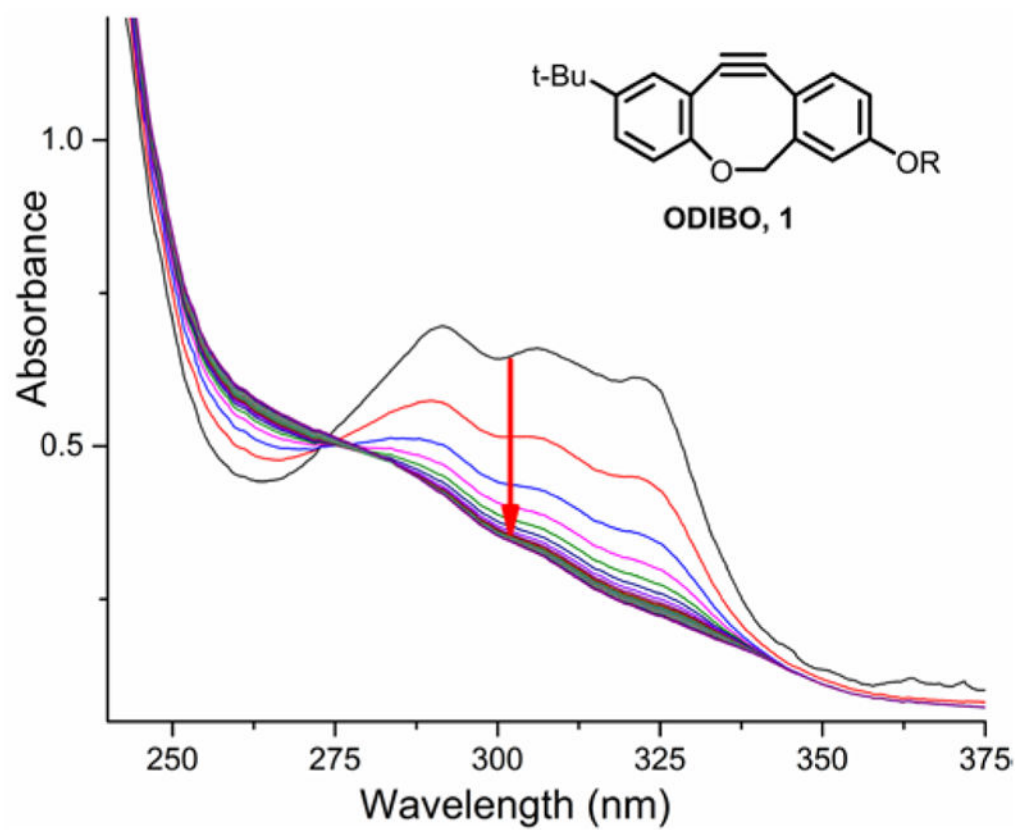


Figure 1. UV spectra showing the loss of the ODIBO (**1**) absorbance peaks during the reaction between ODIBO (0.05 mM) and NaN_3 (2.5 mM) in PBS buffer with 5% methanol. Spectra were recorded every 30 s for 3 min.

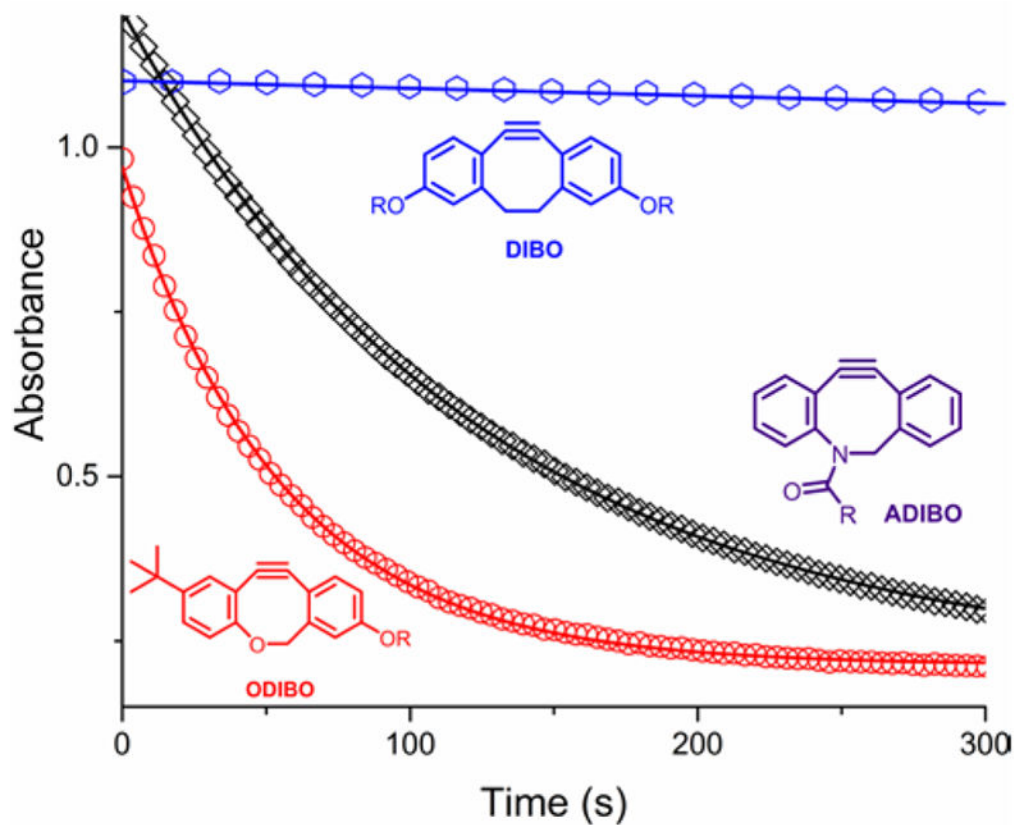


Figure 2. The kinetic traces of the reaction of ODIBO (1, red circles), ADIBO (2, black squares), and DIBO (3a, blue hexagons) with 2.5 mM sodium azide in PBS buffer. The curves represent the least squares fits of a single exponential decay model to the data, yielding a quasi-first order decay constant k_{obs} for each curve.

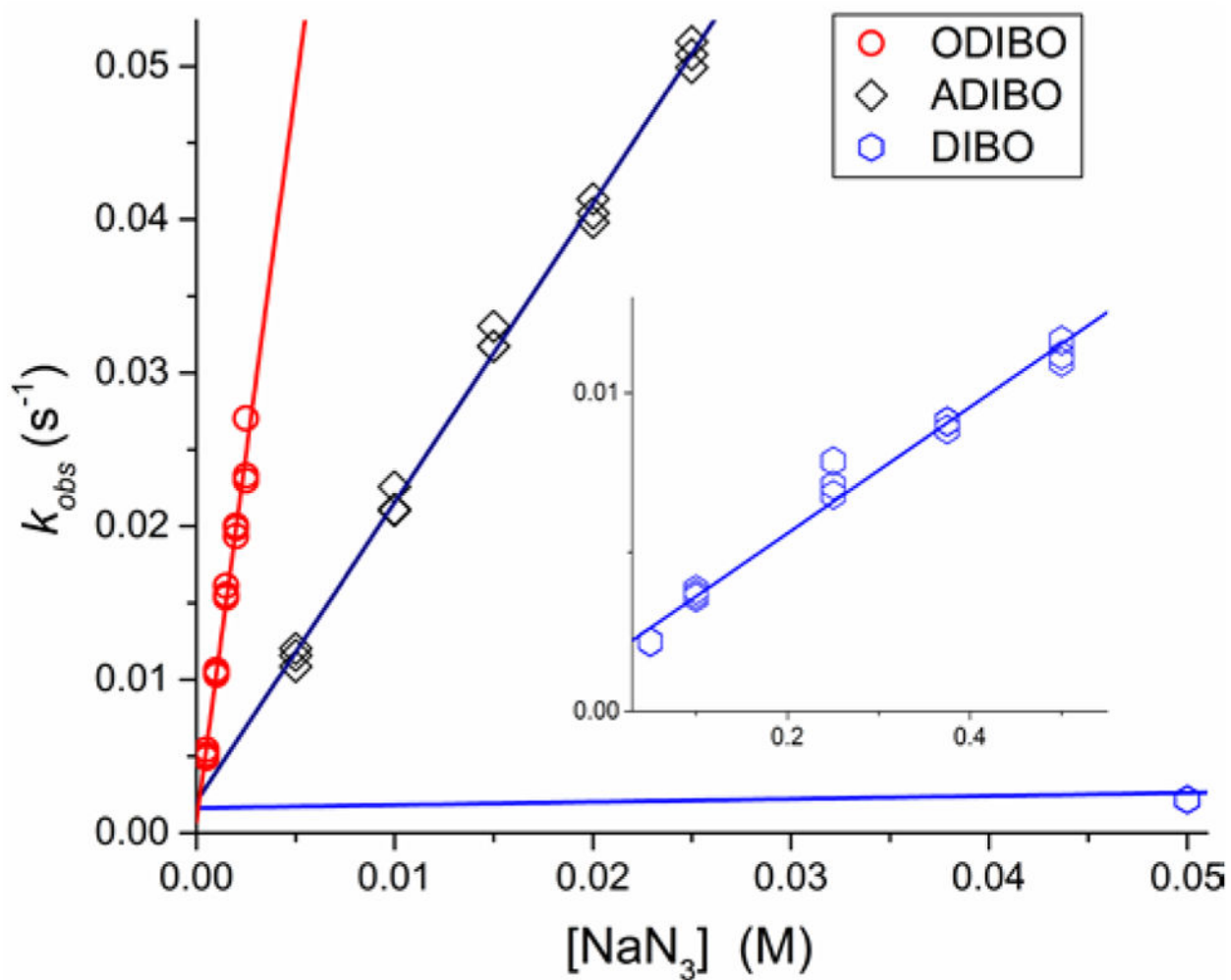


Figure 3. Linear dependence of the observed rates, k_{obs} , of the reaction of ODIBO (1, circles), ADIBO (2, squares), and DIBO (3a, hexagons) on sodium azide concentration in PBS buffer (pH=7.4). The insert shows rate data for DIBO over the broader range of NaN_3 concentrations.

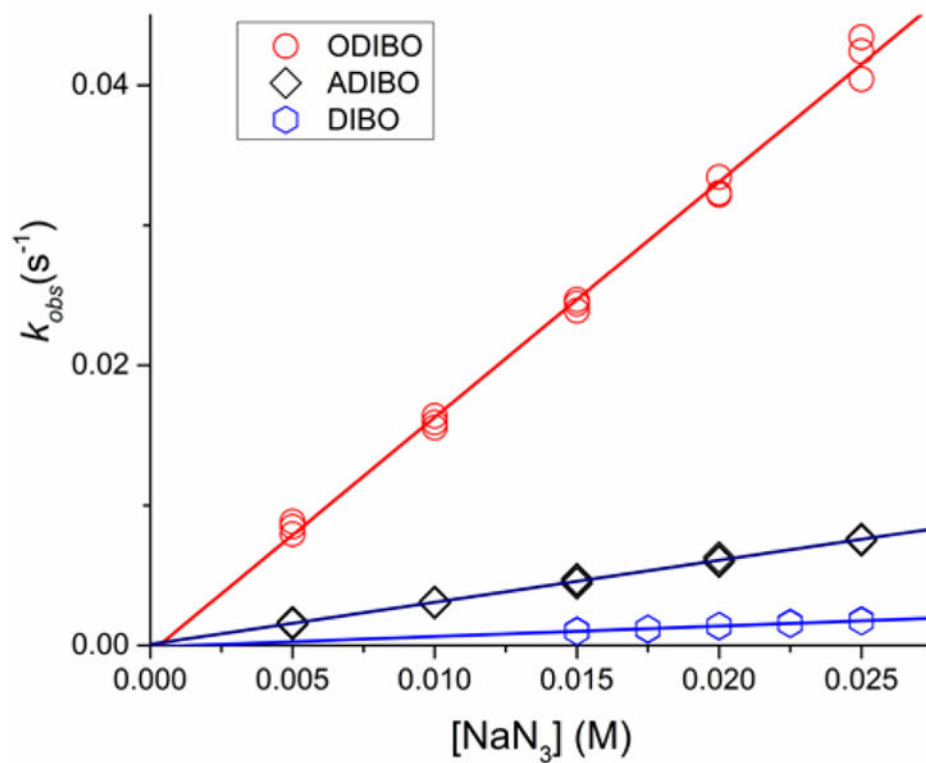


Figure 4. Dependence of the observed rates, k_{obs} , of the reaction of ODIBO (**1**, circles), ADIBO (**2**, squares), and DIBO (**3a**, hexagons) on sodium azide concentration in 0.1 M perchloric acid.

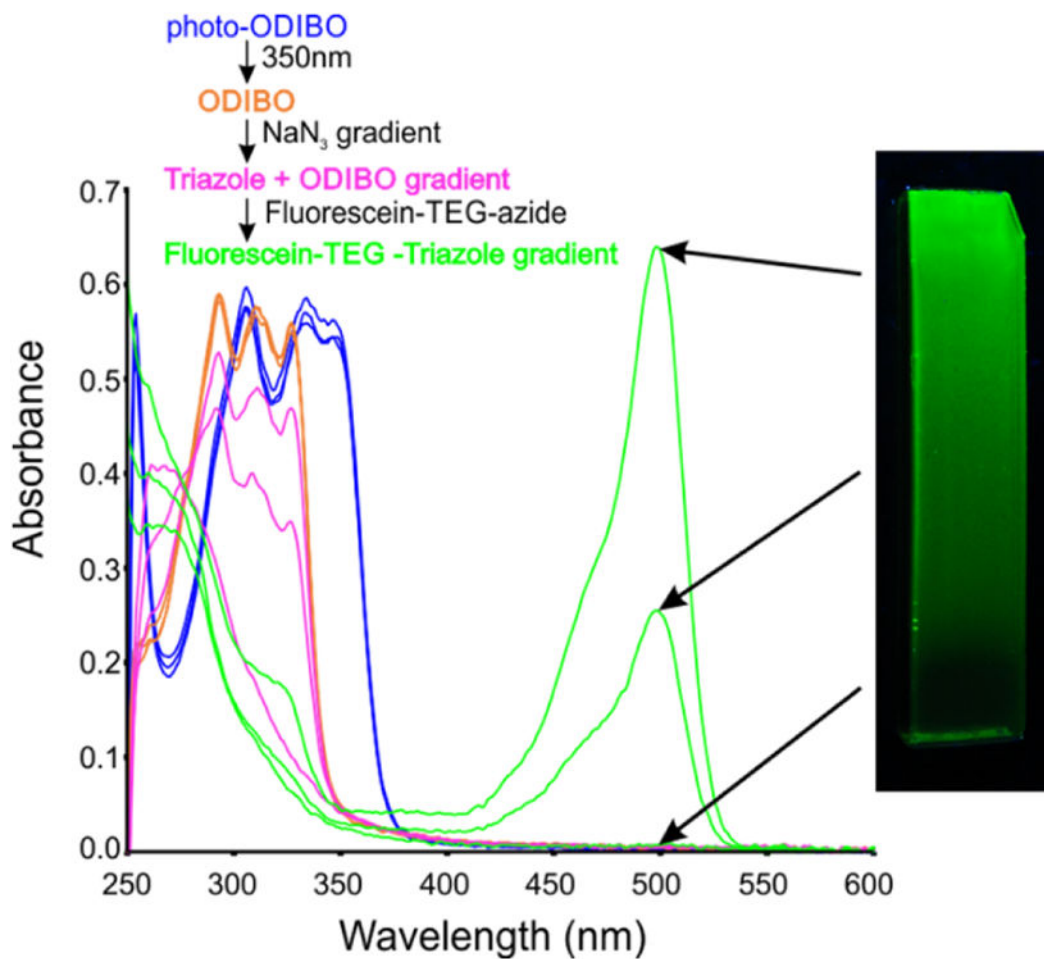


Figure 5. Gradient quenching of a uniform field of ODIBO in a hydrogel following localized application of sodium azide to the base of the hydrogel. The absorbance spectrum of the hydrogel was measured along the gel at various stages of the experiment demonstrating conversion of the initially uniform field of photo-ODIBO into a uniform field of ODIBO, followed by the graded quenching of the ODIBO, yielding the final gradient of fluorescein along the hydrogel.

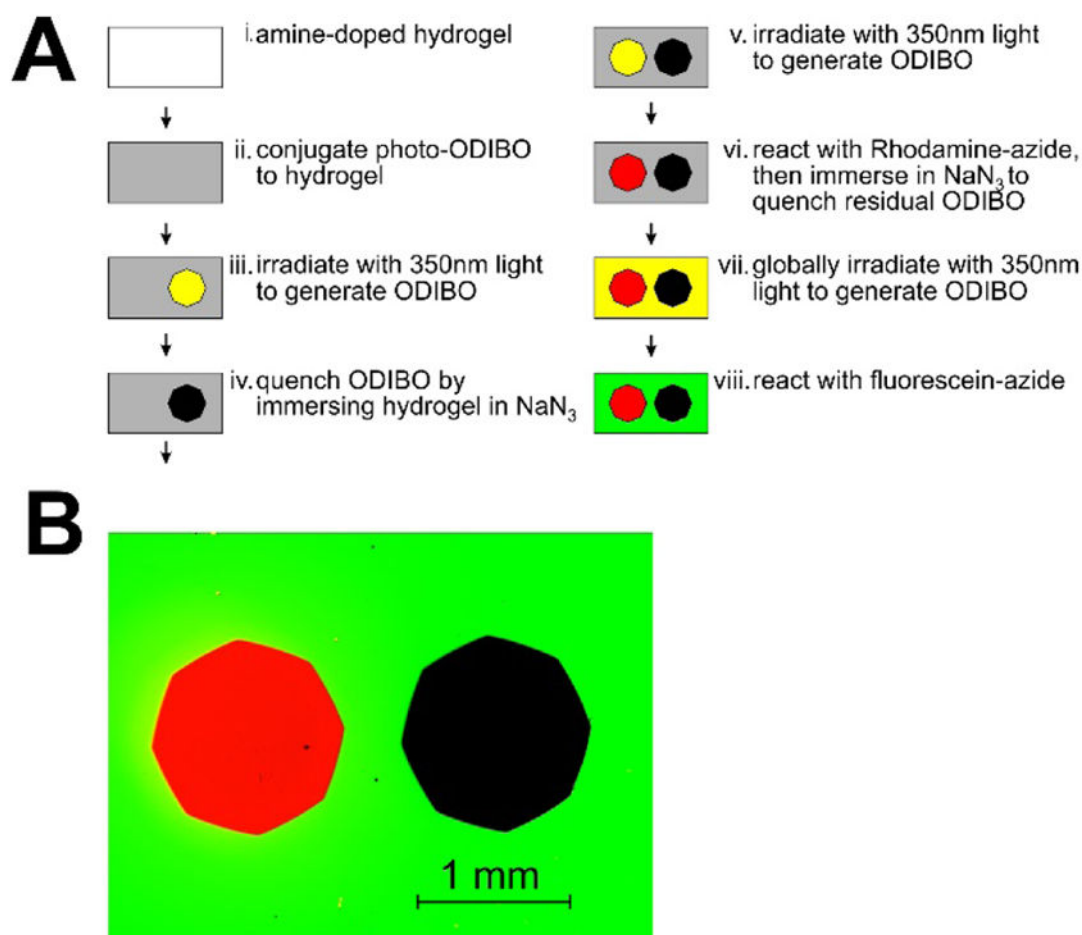
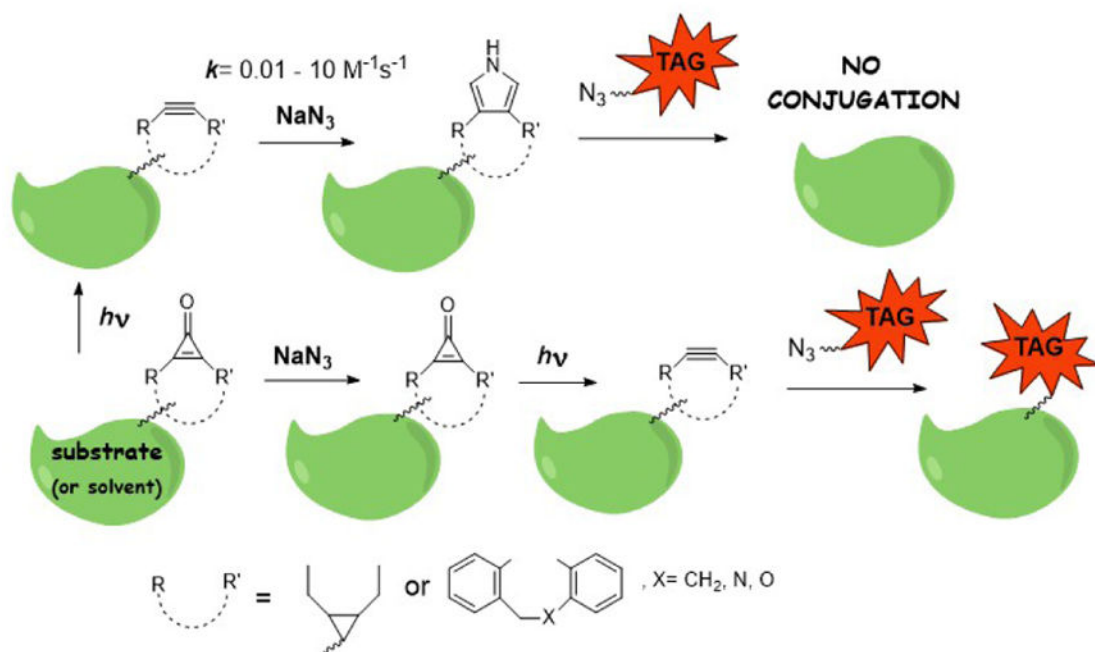
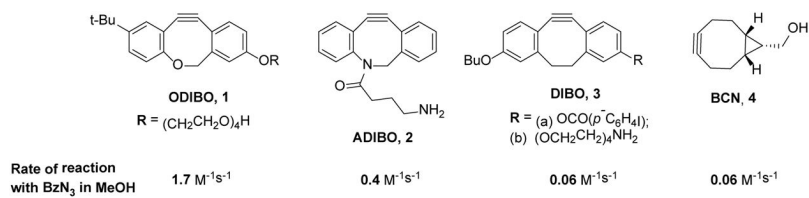


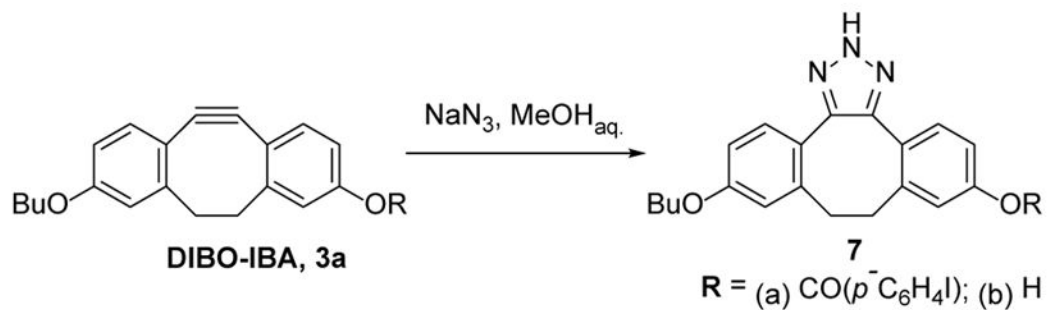
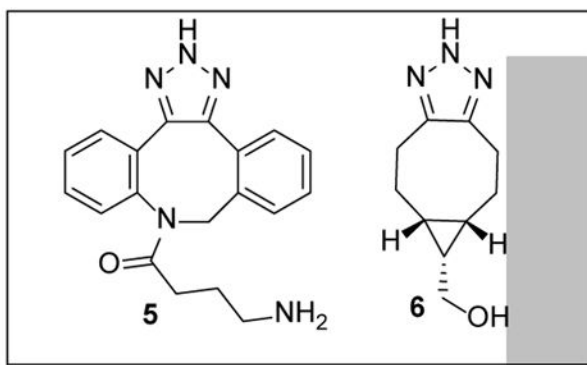
Figure 6. Photopatterning of a uniform field of photo-ODIBO in a hydrogel using a sequence of projected images of an iris diaphragm at 350 nm. A) The black spot was generated by quenching the first image with NaN_3 . The red spot by reacting the second image with Rhodamine B-azide. The green background by reacting with 6-carboxyfluorescein-TEG azide following a final global exposure to 350 nm light. B) Image of the resulting labeled hydrogel.

**Scheme 1.**

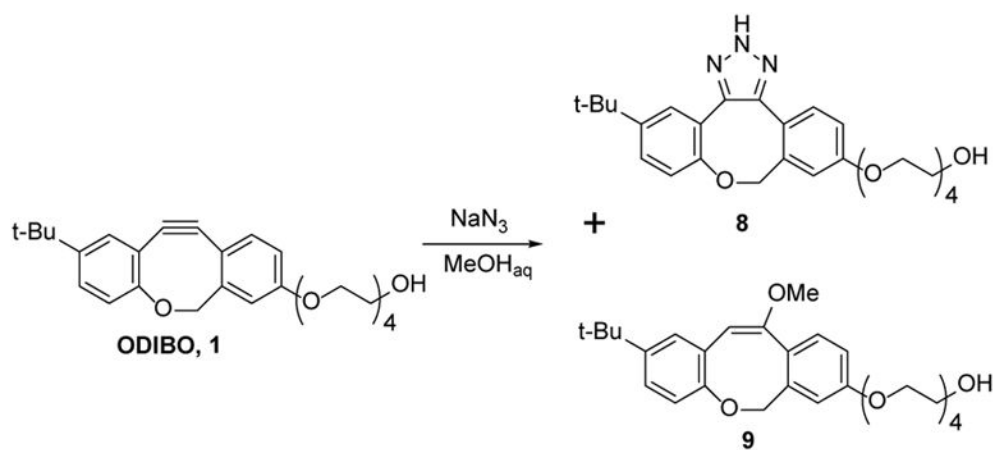
Selective quenching of cyclooctynes with sodium azide in the presence of cyclopropanones.

**Scheme 2.**

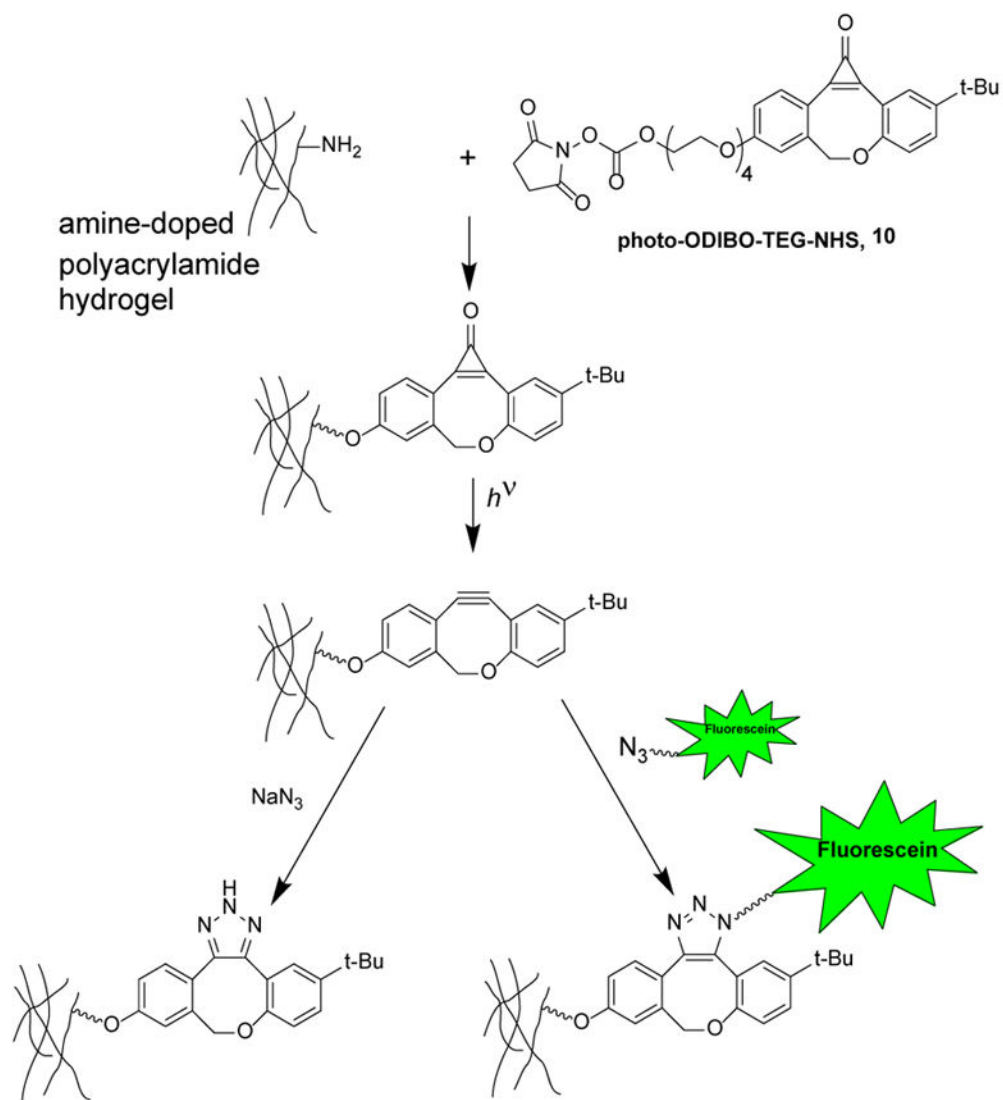
Relative reactivity of common SPAAC reagents towards organic azides.

**Scheme 3.**

2H-Triazoles formed in the reaction of cyclooctynes with NaN₃.



Scheme 4.
Reaction of ODIBO with NaN₃ in methanol.



Scheme 5.
Light-selective labeling or quenching of ODIBO linked to a hydrogel.

Table 1

Second order rate constants for the reaction of cyclooctynes with sodium azide (at pH=7.4) and hydrazoic acid (at pH=1)

| Cyclooctyne | Rate of reaction with azide ion ($M^{-1}s^{-1}$) | Rate of reaction with hydrazoic acid ($M^{-1}s^{-1}$) | Rate of reaction with benzyl azide ($M^{-1}s^{-1}$) |
|-----------------------|--|---|---|
| ODIBO (1) | $9.6 \pm 0.4^a)$ | 1.68 ± 0.03 | 1.75 ± 0.04 |
| ADIBO (2) | 1.95 ± 0.03 | 0.299 ± 0.004 | 0.36 ± 0.01 |
| DIBO (3b) | 0.0198 ± 0.0008 | 0.074 ± 0.02 | 0.056 ± 0.003 |
| BCN ^{b)} (4) | 0.009 ± 0.002 | ~ 0.013 | 0.060 ± 0.003 |

^{a)} Standard errors;

^{b)} the rate constants for the reaction of BCN with azide and hydrazoic acid were evaluated by a competition experiment with DIBO¹⁵